16 Aug 2008, 8:45am - 12:30pm

Generating Realistic Ground Motions for Nonlinear Seismic Hazard Analysis — An Application to Hard Rock Sites in Eastern North America

Jale Tezcan

Southern Illinois University-Carbondale, Carbondale, IL

GENERATING REALISTIC GROUND MOTIONS FOR NONLINEAR SEISMIC HAZARD ANALYSIS- AN APPLICATION TO HARD ROCK SITES IN EASTERN NORTH AMERICA

Jale Tezcan
Southern Illinois University-Carbondale
Carbondale, IL-USA 62901

ABSTRACT

This paper aims to determine the dependence of seismic response on the shape of the time-domain filter used in the stochastic method of ground motion prediction. Brune's single-corner point source model was used in conjunction with the current attenuation relationships developed for hard rock sites in the Eastern North America (ENA) to obtain the target ground motion spectrum. A total of three hundred synthetic accelerograms were generated by filtering the Gaussian white noise with exponential, triangular and trapezoidal windows. For each accelerogram, displacement response of the Duffing's oscillator was calculated, and its average amplitude spectrum was constructed in the joint time-frequency domain using Mexican hat wavelets. This procedure was repeated for three levels of nonlinearity. Among the three shapes examined, the trapezoidal window was associated with longer durations of sustained energy, thereby increasing the level of the expected damage. The dependence of the seismic response to the particular filter shape became more pronounced with increased levels of nonlinearity. This study concludes that ground motions with the same Fourier Amplitude Spectrum could cause substantially different levels of seismic damage on the same structure, depending on the time-frequency localization of the energy imparted to the structure.

INTRODUCTION

The stochastic method is a practical tool to predict ground motions for regions like Eastern North America (ENA), where the amount of recorded ground motion data are not sufficient to perform seismic hazard analysis using statistical procedures The stochastic approach generates sample records that are statistically similar to those expected at a given site, due to an earthquake of specified magnitude. The most critical step in the stochastic method is the formulation of the ground motion spectrum, which takes into account the source, path and local site effects. Ground motions compatible with the target spectrum are generated by filtering a zero mean and unit variance Gaussian white noise and windowing the filtered noise in the time domain to control the shape of the resulting ground motion.

At the core of the stochastic method described above, lies the assumption that the ground motion is a stationary random process. This assumption is not realistic, since earthquakes with the same spectra can exhibit a considerable difference in destructiveness depending on the rate of energy input in the time domain (Shinozuka 1970; Drenick 1977). Figure 1 shows two signals with the same frequency content, that exhibit apparent dissimilarity in the time domain. Their

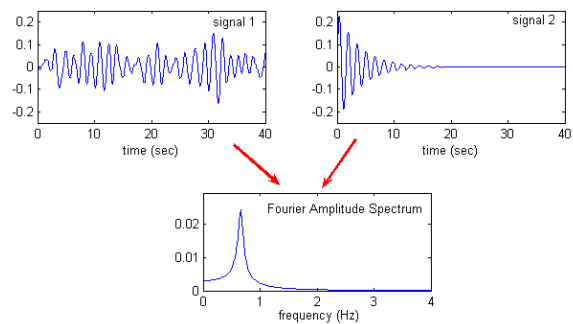Fourier Amplitude Spectra are indistinguishable, since time domain localization is lost.

Fig. 1. Common Fourier Spectra of two signals

Although time domain windowing procedure used in the stochastic method introduces some time dependence into the spectrum, the potential implications of the resulting change on seismic hazard analysis are commonly ignored. Since the selection of the window shape is somewhat arbitrary, the resulting linear response spectra do not seem to be highly sensitive to the shape of the windowing function. Considering that it is not economical to design structures to remain in the linear elastic range during moderate to large earthquakes, it

becomes crucial to investigate the effect of the selected window shape, thus the time dependence of the spectrum, on the response of nonlinear structures.

In this study, a total of three hundred sample accelerograms representing the expected ground motions for hard rock sites in the ENA were generated using using exponential, triangular and trapezoidal windows. The Duffing's oscillator, a classical example in nonlinear vibrations, was used in this study for the response simulations. Duffing's oscillator is a mathematical model representing a Single Degree of Freedom (SDOF) system with cubic nonlinearity in stiffness (Caughey 1963; Iwan 1969). Since the Duffing's oscillator describes the response of several physical systems under harmonic loads, its response has been studied by many researchers (Caughey 1971; Nayfeh and Mook 1979; Roberts and Spanos 1986). Although several method have been developed for special loading conditions, its explicit solutions under general loading conditions do not exist; numerical methods are necessary for time history simulations. This study uses a 4th order Runge-Kutta algorithm for displacement response calculations.

Since the accumulation of seismic damage depends on the time-frequency localization of the energy imparted to the system, the displacement response was transformed to the wavelet domain using the Mexican hat wavelets. The time-frequency patterns observed in the system response for the three windowing functions were investigated, and the effect of system nonlinearity was discussed.

THE GROUND MOTION MODEL

The ground motion spectrum at a given site is often expressed as a product of source, path and local site effects. The Fourier Amplitude Spectrum of the horizontal component of the ground acceleration $F(f)$ is related to the source spectrum, $E(M_0, f)$, path effects, $P(R, f)$, and site effects, $G(f)$, as follows (Boore 2003):

$$F(f) = (2\pi f)^2 \cdot E(M_0, f) \cdot P(R, f) \cdot G(f) \qquad (1)$$

where M_0 (dyne-cm) is the seismic moment, R (km) is the hypocentral distance, $f\,(Hz)$ is the cyclic frequency. The moment magnitude and the seismic moment are related to the moment magnitude through the equation (Aki 1966; Hanks and Kanamori 1979) :

$$M_w = \frac{2}{3}\log_{10} M_0 - 10.7 \qquad (2)$$

The source spectrum $E(M_0, f)$ is given by:

$$E(M_0, f) = c\, M_0\, S(M_0, f) \qquad (3)$$

where $S(M_0, f)$ is the displacement source spectrum and c is the scaling factor defined as (Boore 1983) :

$$c = \frac{R_{\theta\phi}\, V\, F}{4\pi \rho_s \beta_s^{\,3} R_0}. \qquad (4)$$

In Eq.(4), $R_{\theta\phi} = 0.55$ is the average shear wave radiation pattern (Boore and Boatwright 1984), $V = 0.707$ is the partition of the total energy carried by the two horizontal shear wave components, $F = 2$ is the free surface amplification factor, $\rho_s \left(g/cm^3\right)$ and $\beta_s \left(km/s\right)$ are the crustal density and the shear wave velocity in the vicinity of the point source, respectively, and $R_0 = 1$ km is a reference distance.

Proper selection of the source model plays a critical role in ground motion modeling as the displacement source spectrum $S(M_0, f)$ models the frequency distribution of the seismic energy released during an earthquake. When the seismic energy can be assumed to originate from a point source, Brune's point source model can be used to define $S(M_0, f)$ as (Brune 1970):

$$S(M_0, f) = \frac{1}{1 + \left(f / f_0\right)^2}. \qquad (5)$$

Brune's model requires a corner frequency, $f_0 \left(Hz\right)$, which can be calculated from the seismic moment M_0, stress drop $\Delta\sigma$ and the shear wave velocity β_s, using:

$$f_0 = 4.9 \times 10^6 \beta_s \left(\frac{\Delta\sigma}{M_o}\right)^{1/3}. \qquad (6)$$

The path term, $P(R, f)$, in Eq.(1) models the anelastic attenuation and geometric spreading, and is given by:

$$P(M_0, f) = Z(R) \cdot \exp\left(\frac{-\pi f R}{Q(f)\beta_s}\right). \qquad (7)$$

where $Z(R)$ is a trilinear function representing the geometric spreading as a function of the closest distance to the rupture surface, R(km). The $Q(f)$ term accounts for the path dependent attenuation not included in $Z(R)$ term. This paper adopts $Q(f) = 893 f^{0.32}$ (Atkinson 2004). For the Eastern North America (ENA), the geometric spreading function is (Atkinson and Boore 1995; Frankel, Mueller et al. 1996):

$$Z(R) = \begin{cases} \dfrac{1}{R} & R \le 70 \ km \\[2mm] \dfrac{1}{70} & 70 \ km \le R \le 130 \ km \\[2mm] \dfrac{1}{170}\sqrt{\dfrac{130}{R}} & R > 130 \ km \end{cases} \quad (8)$$

The site term $G(f)$ in Eq.(1) accounts for the local amplification $A(f)$ and diminution $D(f)$ effects, and is given by:

$$G(f) = A(f)D(f) \quad (9)$$

When shear waves move from the bedrock to softer soil, their propagation velocity decreases as a response to the decreased elastic modulus, amplifying the ground motion. This increase is modeled by frequency dependent amplification factors, which can be calculated by the quarter wavelength method (Joyner and Boore 1981; Campbell 2003). Table 1 shows the amplification factors adopted in the study, which are derived for hard rock sites in the ENA (Atkinson and Boore 2006).

Table 1 Site Amplification factors for NEHRP A (Atkinson and Boore 2006)

Frequency f (Hz)	Amplification Factor $A(f)$
0.5	1.00
1	1.13
2	1.22
5	1.36
10	1.41
50	1.41

The diminution function $D(f)$ in Eq. (9) is a low-pass filter representing the spectral amplitude reduction observed at high frequencies. This reduction is commonly modeled either using the kappa parameter, κ, which relates the damping with the shear wave velocity over the soil column, or defining a cutoff frequency f_{max} (Hanks 1982). The parameter κ is the slope of the log spectra versus frequency curve (Anderson and Hough 1984):

$$D(f) = e^{-\pi \kappa f} \quad (10)$$

For hard rock sites in ENA, the kappa parameter has little influence on the simulation results for high frequencies (Atkinson and Boore 2006). To induce a sharp decrease in the spectral amplitudes after a cutoff frequency f_{max}, the diminution function can be defined as (Boore 1986):

$$D(f) = \frac{1}{\sqrt{1 + \left(\dfrac{f}{f_{max}}\right)^8}}. \quad (11)$$

The cutoff frequency used in this study, is given in Table 2, where the ground motion parameters are listed.

Table 2 Ground motion parameters used in this study

Parameter	Value
Magnitude, M	7
Stress drop, $\Delta\sigma$	150 bars
Hypocentral distance, R	10 km
Crustal density, ρ_s	2.8 g/cm^3
Shear wave velocity, β_s	3.7 km/s
Cut-off frequency, f_{max}	50 Hz.

GENERATION OF SPECTRUM-COMPATIBLE ACCELEROGRAMS

Three sets of one-hundred time series were generated by filtering zero- mean and unit-variance Gaussian white noise. The series were multiplied by one of the three windowing functions: exponential (g_1), triangular (g_2) and trapezoidal (g_3). Figure 2 shows the windowing functions used.

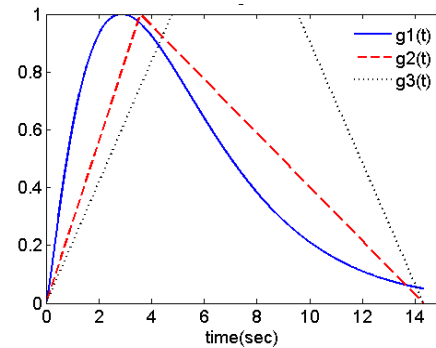*Fig. 2. Time domain windowing functions*

The functions $g_1(t)$, $g_2(t)$, and $g_3(t)$ are defined as:

$$g_1(t) = at^b e^{-ct} \quad (12)$$

$$g_2(t) = \begin{cases} \dfrac{4t}{T} & t \le \dfrac{T}{4} \\[3mm] 1 - \dfrac{4}{3T}\left(t - \dfrac{T}{4}\right) & t > \dfrac{T}{4} \end{cases} \quad (13)$$

$$g_3(t) = \begin{cases} \dfrac{3t}{T} & t \le \dfrac{T}{3} \\ 1 & \dfrac{T}{3} < t \le \dfrac{2T}{3} \\ 1 - \dfrac{3}{T}\left(t - \dfrac{2T}{3}\right) & t > \dfrac{2T}{3} \end{cases} \qquad (14)$$

The parameters a, b and c in Eq. (12) are related to the duration and the peak amplitude of the window. The duration, T is taken as twice the sum of source duration T_s and path duration T_p (Boore 1983):

$$T = 2(T_s + T_p) \qquad (15)$$

The source duration is the inverse of the corner frequency f_0:

$$T_s = \frac{1}{f_0} \qquad (16)$$

and the path duration is (Atkinson and Boore 1995):

$$T_p = \begin{cases} 0 & R \le 10 \ km \\ 0.16(R-10) & 10 \ km \le R \le 70 \ km \\ 9.6 - 0.03(R-70) & 70 \ km \le R \le 130 \ km \\ 7.8 + 0.04(R-130) & R > 130 \ km \end{cases} \qquad (17)$$

All accelerograms in this study have the same duration, since the magnitude and distance were kept constant.

Next, each time series was transformed to the frequency domain, and its Fourier spectrum was scaled to fit the target spectrum. Finally, the scaled Fourier amplitude spectrum was transformed back to the time domain by inverse Fourier Transform to produce the sample ground motion record.

Figure 3 shows the convergence of the simulation results to the target spectrum, as the sample size is increased. The simulation results show that the Fourier amplitude spectrum averaged over one hundred samples, successfully matches the target spectrum. Only the results from the exponential windowing are shown, the other two cases produced similar results.
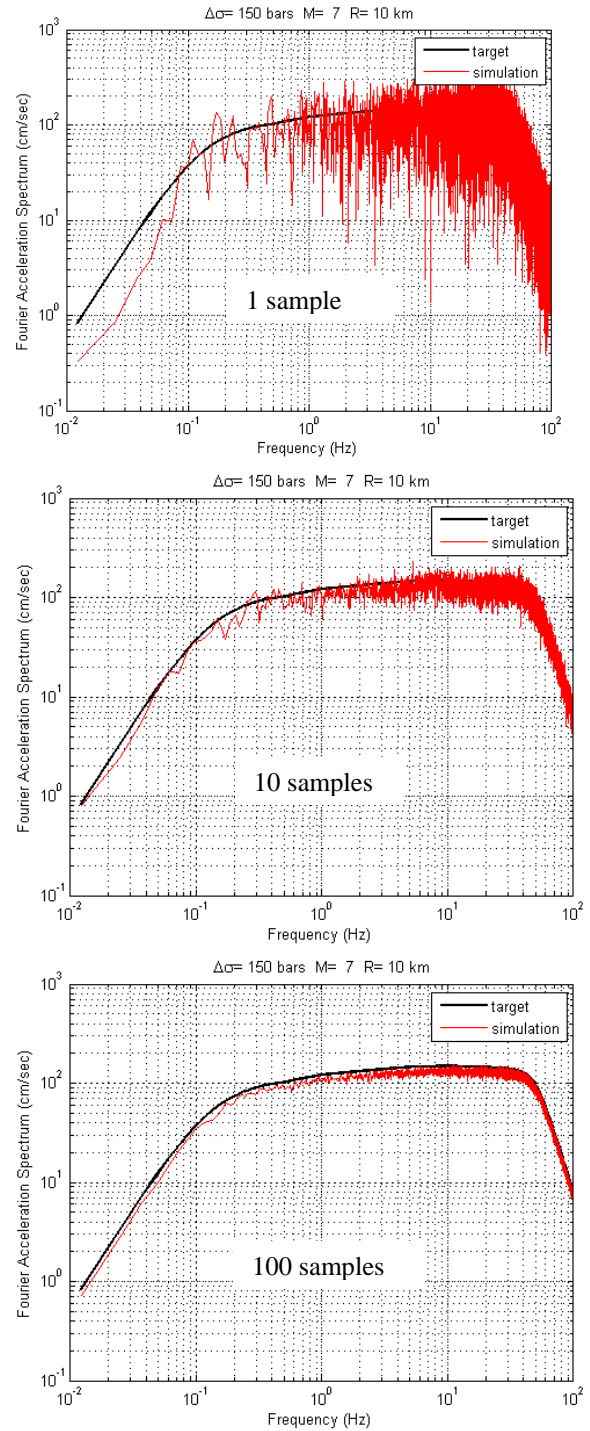

Fig. 3. Target and simulated spectra using 1, 10 and 100 samples with an exponential window

CALCULATION OF THE SYSTEM RESPONSE

This paper considers the Duffing's oscillator with the following equation of motion:

$$\ddot{x} + 2\zeta\omega_n\dot{x} + \omega_n^2 x + \lambda x^3 = f(t) \qquad (18)$$

where λ is the nonlinearity parameter and ζ and ω_n are the damping ratio and the natural frequency of the corresponding linear system, i.e. when $\lambda = 0$.

The damping ratio and the natural frequency were kept constant at $\zeta = 5\%$ and $\omega_n = 2\pi$ $radians$, while the nonlinearity parameter took the values $\lambda = 0, 1$ and 5. Figure 4 shows the target ground motion spectrum, and the unscaled frequency response function.
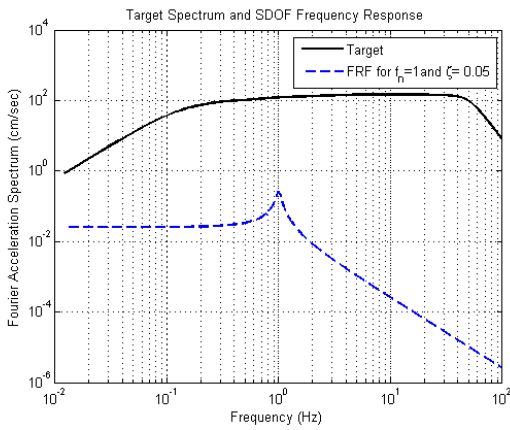
Fig. 4. Target Spectrum and the Frequency Response Function (FRF) of the linear SDOF system

For each of the three windowing functions, one hundred sample records were generated, and the solution of Eq (18) was found for the cases of $\lambda = 0$, $\lambda = 1$ and $\lambda = 5$ using a 4th order Runge-Kutta algorithm.

Figure 5, Fig. 6 and Fig. 7 show typical displacement time histories for samples filtered with the exponential, triangular and trapezoidal windows, respectively.
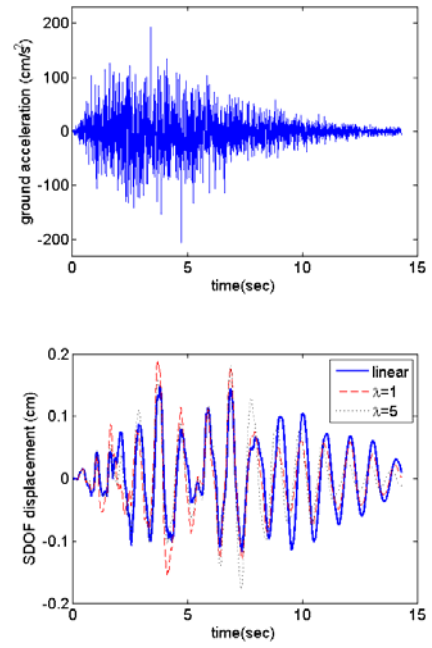
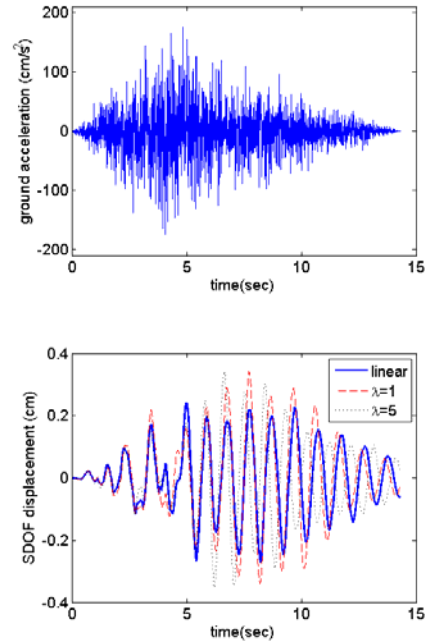Fig. 5. Ground acceleration and displacement response for the exponential window

Fig. 6. Ground acceleration and displacement response for the triangular window
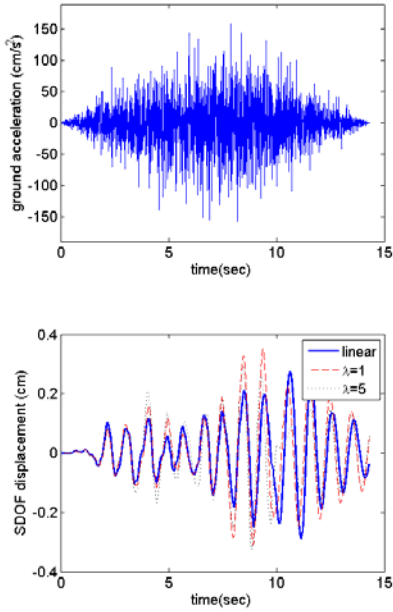
Fig. 7. Ground acceleration and displacement response for the trapezoidal window

Comparison of the maximum displacement amplitudes indicates that the nonlinear system response exceeds the linear system response, sometimes by a factor of 1.3. Since the system has cubic hardening effect when $\lambda = 1$ or $\lambda = 5$, this result may seem counterintuitive. However, nonlinear phenomena, such as bifurcation and jump phenomenon explain the observed behavior of the Duffing's oscillator. It has been shown that the maximum amplitude of the Duffing's oscillator can be several times larger than that predicted by linear theory. (Yang, Nayfeh et al. 1998).

The deviation from the linear response for all the three cases, becomes more pronounced with increased displacement response. Among the three filter shapes, the exponential window, as *Fig. 5* shows, presents the case where the effect of nonlinearity is the smallest. For the triangular case, as shown in *Fig. 6*, the high deviation from the linear case is mostly limited to the mid one-third region of the displacement history. In the case of the trapezoidal window, *Fig. 7*, the deviation is still remarkable in the last one-third region of the time history.

WAVELET ANALYSIS OF THE RESPONSE

The wavelet transform decomposes a signal $x(t)$ into basis functions that are dilations and translations of the mother wavelet $\psi(t)$ through the convolution (Daubhechies 1992; Meyer 1992):

$$W_\psi x(a,b) = \frac{1}{\sqrt{a}} \int_{-\infty}^{\infty} x(t) \psi^*(\frac{t-b}{a}) dt \qquad (19)$$

where ψ^* is the complex conjugate of the wavelet, a and b are the scale and the time parameters of the wavelet, respectively. The coefficients $W_\psi x(a,b)$ measure the similarity between the signal and the scaled and translated wavelet, $\psi(\frac{t-b}{a})$. The square of the wavelet coefficient $\left|W_\psi x(a,b)\right|^2$ is proportional to energy of $x(t)$ contained in the time-frequency grid represented by the scaled and translated wavelet (Spanos, Tezcan et al. 2005).

This study uses the Mexican hat wavelet, a frequently used wavelet in modeling seismic data., The Mexican hat wavelet is very efficient for time-frequency decomposition of the ground motion from a single source rupture (Zhou and Adeli 2003). Figure 8 shows the Mexican hat wavelet function, which is the second derivative of the Gaussian probability density function (Daubhechies 1992):

$$\psi(t) = \left(\frac{2}{\sqrt{3}} \pi^{-1/4}\right)\left(1 - t^2\right) e^{-t^2/2} . \qquad (20)$$
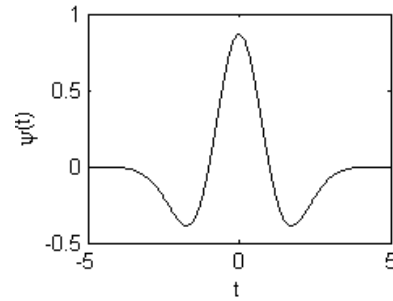

Fig. 8. Mexican hat wavelet function

Wavelet coefficients of the displacement response, discussed in the previous section, were computed using the Mexican hat wavelet., Wavelet amplitude spectra of the displacement response, averaged over one hundred realizations, corresponding to accelerograms filtered with exponential, triangular and trapezoidal windows are shown in Fig. 9, Fig. 10 and Fig. 11, respectively.

Examination of the time domain behavior of the amplitude spectra, supports the discussions presented in the previous section. In the frequency domain, for all cases, the earthquake energy is concentrated around $f = 1\,Hz.$, which is the chosen undamped natural frequency of vibration of the system. A closer examination reveals an upward shift in the frequency level where the energy is concentrated, for the two nonlinear cases, $\lambda = 1$ and $\lambda = 5$. As expected, this shift is more apparent for the higher nonlinearity case, $\lambda = 5$.
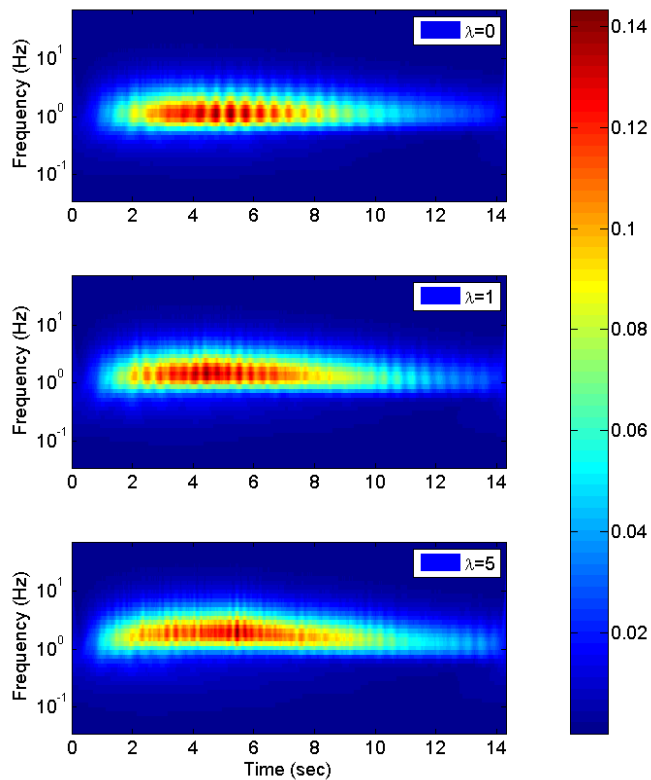
Fig. 9. Wavelet amplitude spectra of the displacement response for $\lambda = 0$, $\lambda = 1$ and $\lambda = 5$ using exponential window.
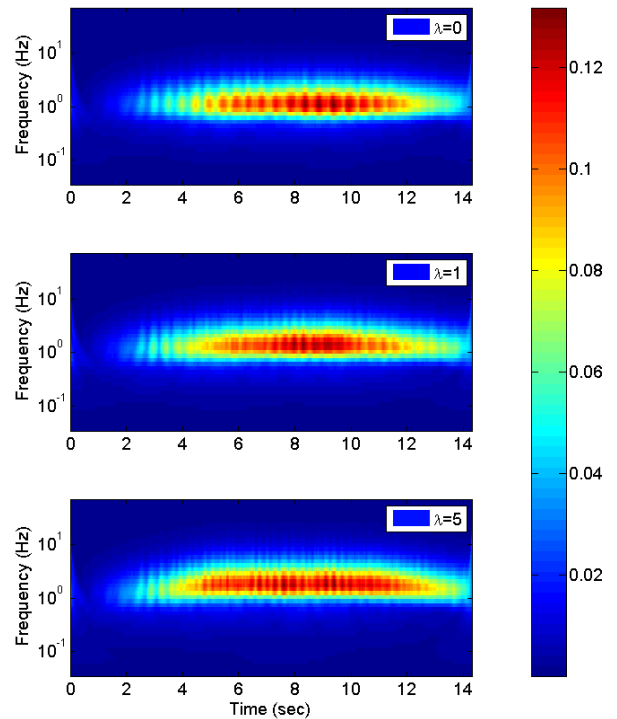

Fig. 10. Wavelet amplitude spectra of the displacement response for $\lambda = 0$, $\lambda = 1$ and $\lambda = 5$ using triangular window.

Fig. 11. Wavelet amplitude spectra of the displacement response for $\lambda = 0$, $\lambda = 1$ and $\lambda = 5$ using the trapezoidal window.
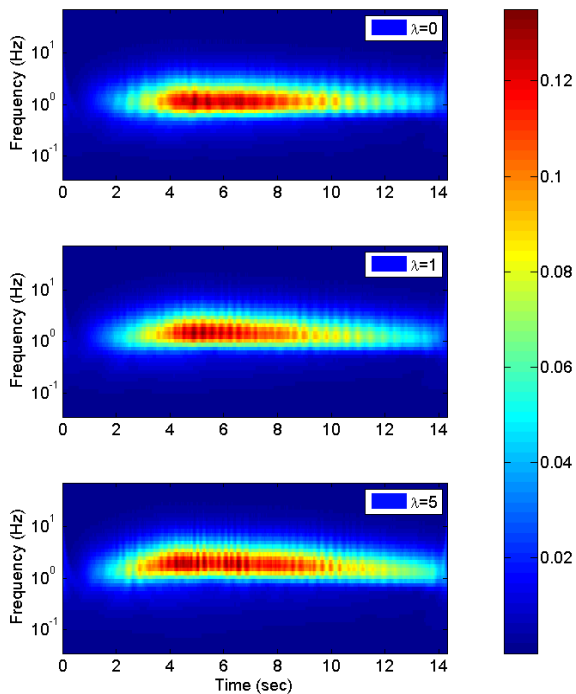
CONCLUSION

This study investigates the dependence of the system response on particular shape of the windowing function used in the stochastic method of ground motion generation. Three sets of one-hundred synthetic time series, that are compatible with a target spectrum representing the hard rock sites in the Eastern North America (ENA), were generated by filtering white noise using one of the three windowing functions: exponential, triangular and trapezoidal. For each accelerogram, the displacement history of the Duffing's oscillator, a classical example in nonlinear vibrations, was calculated using a 4th order Runge-Kutta algorithm. To observe the time-frequency localization of the earthquake energy, the system response is mapped to the wavelet domain using Mexican hat wavelets. The effect of the window shape on structural response for different levels of nonlinearity was discussed.

Analysis results indicate that responses to accelerograms matching a certain target spectrum can have different energy localization patterns. Among the three windows used in this study, the trapezoidal window was associated with longer durations of sustained energy, potentially causing increased numbers of strain reversals, ultimately increasing the level of the expected damage. The Duffing's system with stronger nonlinearity was more sensitive to particular shape of the windowing function, presenting additional challenges to their seismic performance assessment.

REFERENCES

Aki, K. [1966]. "Generation and propagation of G waves from the Niigata earthquake of June 16, 1964. Part 2. Estimation of earthquake moment, released energy, and stress-strain drop from the G wave spectrum." Bull. Earthquake Res. Inst., Tokyo Univ 44: 73-88.

Anderson, J. G. and S. E. Hough [1984]. "A model for the shape of the fourier amplitude spectrum of acceleration at high frequencies." Bulletin of the Seismological Society of America 74(5): 1969-1993.

Atkinson, G. M. [2004]. "Empirical Attenuation of Ground-Motion Spectral Amplitudes in Southeastern Canada and the Northeastern United States." Bulletin of the Seismological Society of America 94(3): 1079-1095.

Atkinson, G. M. and D. M. Boore [1995]. "Ground-motion relations for eastern North America." Bulletin of the Seismological Society of America 85(1): 17-30.

Atkinson, G. M. and D. M. Boore [2006]. "Earthquake Ground-Motion Prediction Equations for Eastern North America." Bulletin of the Seismological Society of America 96(6): 2181-2205.

Boore, D. M. [1983]. "Stochastic simulation of high-frequency ground motions based on seismological models of the radiated spectra." Bulletin of the Seismological Society of America 73(6 A): 1865-1894.

Boore, D. M. [1986]. "Short-period P-and S-wave radiation from large earthquakes: Implications for spectral scaling relations." Bulletin of the Seismological Society of America 76(1): 43-64.

Boore, D. M. [2003]. "Simulation of Ground Motion Using the Stochastic Method." Pure and Applied Geophysics 160(3): 635-676.

Boore, D. M. and J. Boatwright [1984]. "Average body-wave radiation coefficients." Bulletin of the Seismological Society of America 74(5): 1615-1621.

Brune, J. N. [1970]. "Tectonic stress and the spectra of seismic shear waves from earthquakes." J. Geophys. Res 75(26): 4997-5009.

Campbell, K. W. [2003]. "Prediction of Strong Ground Motion Using the Hybrid Empirical Method and Its Use in the Development of Ground-Motion (Attenuation) Relations in Eastern North America." Bulletin of the Seismological Society of America 93(3): 1012-1033.

Caughey, T. K. [1963]. "Equivalent Linearization Techniques." Journal of the Acoustical Society of America 35(11): 1706-1711.

Caughey, T. K. [1971]. "Nonlinear Theory of Random Vibrations." Advanced Applied Mechanics 11: 209-253.

Daubhechies, I. [1992]. *"Ten Lectures on Wavelets"*. Philadelphia, PA.

Drenick, R. F. [1977]. "The critical excitation of nonlinear systems." American Society of Mechanical Engineers, Applied Mechanics.

Frankel, A., C. Mueller, et al. [1996]. "National seismic hazard maps, June 1996 documentation." US Geol. Surv. Open-File Rep. 96 532: 110.

Hanks, T. C. [1982]. "f max." Bulletin of the Seismological Society of America 72(6 A): 1867-1879.

Hanks, T. C. and H. Kanamori [1979]. "A moment magnitude scale." J. Geophys. Res 84(2): 348–350.

Iwan, W. D. [1969]. "On Defining Equivalent Systems for Certain Ordinary Nonlinear Differential Equations." International Journal of Nonlinear Mechanics 4: 325-334.

Joyner, W. B. and D. M. Boore [1981]. "Peak horizontal acceleration and velocity from strong-motion records including records from the 1979 imperial valley, California, earthquake." Bulletin of the Seismological Society of America 71(6): 2011-2038.

Meyer, Y. [1992]. *"Wavelets and Operators"*. New York, Cambridge University Press.

Nayfeh, A. H. and D. T. Mook [1979]. *"Nonlinear Oscillations"*. New York, John Wiley.

Roberts, J. and P. D. Spanos [1986]. *"Random Vibration and Statistical Linearization"*. New York, Wiley.

Shinozuka, M. [1970]. "Maximum Structural Response to Seismic Excitations." Journal of the Engineering Mechanics Division 96(5): 729-738.

Spanos, P. D., J. Tezcan, et al. [2005]. "Stochastic processes evolutionary spectrum estimation via harmonic wavelets." Computer methods in applied mechanics and engineering 194(12-16): 1367-1383.

Yang, S., A. H. Nayfeh, et al. [1998]. "Combination resonances in the response of the duffing oscillator to a three-frequency excitation", Springer. 131: 235-245.

Zhou, Z. and H. Adeli [2003]. "Wavelet energy spectrum for time-frequency localization of earthquake energy". 13: 133-140.